Electronic Supplementary Material (ESI) for Analyst.

Screening Natural Libraries of Human Milk Oligosaccharides Against Lectins Using CaR-ESI-MS

Amr El-Hawiet,[1,2] Yajie Chen,[1] Km Shams-Ud-Doha,[1,§] Elena N. Kitova,[1] Pavel I. Kitov,[1] Lars Bode,[3] Naim Hage,[4] Franco H. Falcone[4] and John S. Klassen[1*]

[1]*Alberta Glycomics Centre and Department of Chemistry, University of Alberta, Edmonton, Alberta, Canada T6G 2G2*

[2]*Department of Pharmacognosy, Faculty of Pharmacy, Alexandria University, Alexandria, Egypt*

[3] *Division of Neonatology and Division of Gastroenterology and Nutrition, Department of Pediatrics, and Larsson-Rosenquist Foundation Mother-Milk-Infant Center of Research Excellence, University of California San Diego, CA*

[4]*School of Pharmacy, Division of Molecular Therapeutics and Formulation, University of Nottingham, Nottingham, United Kingdom, NG7 2RD*

* Corresponding Author:

Department of Chemistry

University of Alberta

Edmonton, AB CANADA T6G 2G2

Email: john.klassen@ualberta.ca

Telephone: (780) 492-3501

Fax: (780) 492 8231

§ *Current address: Sanford Burnham Prebys Medical Discovery Institute, 10901 North Torrey Pines Road, La Jolla, California 92037 USA*

Experimental

ESI-MS affinity measurements

Association constants (K_a) for the binding of BabA to each of **HMO1-HMO4**, **HMO6**, **HMO7**, **HMO9** and **HMO18** were measured using the direct ESI-MS assay.[S1,S2] The reported affinities are averages of six replicate measurements performed at a minimum of two different protein/HMO concentrations. All mass spectra were corrected for the occurrence of nonspecific HMO-protein binding during the ESI process using the reference protein method.[S3] The value of K_a was calculated from the measured abundance ratio (R) of the HMO-bound (PL)-to-free protein (P) ions, following correction for nonspecific HMO binding, and the initial concentration of protein ($[P]_0$) and ligand ($[L]_0$), eq S1:

$$K_a = \frac{R}{[L]_0 - \frac{R}{1+R}[P]_0} \quad \text{(S1)}$$

where R is assumed to be equal to the concentration ratio ([PL]/[P]) in solution, eq S2:

$$R = \frac{\sum Ab(PL)}{\sum Ab(P)} = \frac{[PL]}{[P]} \quad \text{(S2)}$$

The ESI-MS affinity measurements were performed in positive ion mode on a Synapt G2S quadrupole-ion mobility separation-time of flight (Q-IMS-TOF) mass spectrometer (Waters, Manchester, UK) equipped with a nanoflow ESI (nanoESI) source. NanoESI tips with ~5 μm outer diameters (o.d.) were produced from borosilicate capillaries (1.0 mm o.d., 0.68 mm inner diameter) using a P-1000 micropipette puller (Sutter Instruments, Novato, CA). To perform nanoESI, a platinum wire was inserted into the sample solution and a voltage of ~1 kV was applied. The Source temperature was 60 °C and the Cone voltage was 50 V; the Trap and Transfer voltages were 5 V and 2 V, respectively. All other instrumental conditions were set to

the default parameters. Data acquisition and processing were performed using MassLynx (Waters, version 4.1).

Table S1. List of MWs, chemical structures and common names of purified HMOs (**HMO1-HMO31**).

HMO	MW (Da)	Structure	Common name
HMO1	488.17	α-L-Fuc-(1→2)-β-D-Gal-(1→4)-β-D-Glc	2'-Fucosyllactose
HMO2	488.17	β-D-Gal-(1→4)-[α-L-Fuc-(1→3)]-β-D-Glc	3-Fucosyllactose
HMO3	633.21	α-D-Neu5Ac-(2→3)-β-D-Gal-(1→4)-β-D-Glc	3'-Sialyllactose
HMO4	633.21	α-D-Neu5Ac-(2→6)-β-D-Gal-(1→4)-β-D-Glc	6'-Sialyllactose
HMO5	634.23	α-L-Fuc-(1→2)-β-D-Gal-(1→4)-[α-L-Fuc-(1→3)]-β-D-Glc	Difucosyllactose
HMO6	707.25	β-D-Gal-(1→3)-β-D-GlcNAc-(1→3)-β-D-Gal-(1→4)-β-D-Glc	Lacto-N-tetraose
HMO7	707.25	β-D-Gal-(1→4)-β-D-GlcNAc-(1→3)-β-D-Gal-(1→4)-β-D-Glc	Lacto-N-neotetraose
HMO8	779.27	α-D-Neu5Ac-(2→3)-β-D-Gal-(1→4)-[α-L-Fuc-(1→3)]-β-D-Glc	3'-Sialyl-3'-fucosyllactose
HMO9	853.31	α- L-Fuc-(1→2)-β-D-Gal-(1→3)-β-D-GlcNAc-(1→3)-β-D-Gal-(1→4)-β-D-Glc	Lacto-N-fucopentaose I
HMO10	853.31	β-D-Gal-(1→3)-[α-L-Fuc-(1→4)]-β-D-GlcNAc-(1→3)-β-D-Gal-(1→4)-β-D-Glc	Lacto-N-fucopentaose II
HMO11	853.31	β-D-Gal-(1→4)-[α-L-Fuc-(1→3)]-β-D-GlcNAc-(1→3)-β-D-Gal-(1→4)-β-D-Glc	Lacto-N-fucopentaose III
HMO12	853.31	β-D-Gal-(1→3)-β-D-GlcNAc-(1→3)-β-D-Gal-(1→4)-[α-L-Fuc-(1→3)]-β-D-Glc	Lacto-N-neofucopentaose V
HMO13	853.31	β-D-Gal-(1→4)-β-D-GlcNAc-(1→3)-β-D-Gal-(1→4)[α-L-Fuc-(1→3)]-β-D-Glc	Lacto-N-neofucopentaose
HMO14	998.34	α-D-Neu5Ac-(2→3)-β-D-Gal-(1→3)-β-D-GlcNAc-(1→3)-β-D-Gal-(1→4)-β-D-Glc	Sialyllacto-N-tetraose a
HMO15	998.34	α-D-Neu5Ac-(2→6)-[β-D-Gal-(1→3)]-β-D-GlcNAc-(1→3)-β-D-Gal-(1→4)- β-D-Glc	Sialyllacto-N-tetraose b
HMO16	998.34	α-D-Neu5Ac-(2→6)-β-D-Gal-(1→4)-β-D-GlcNAc-(1→3)-β-D-Gal-(1→4)-β-D-Glc	Sialyllacto-N-tetraose c
HMO17	998.34	α-D-Neu5Ac-(2→3)-β-D-Gal-(1→4)-β-D-GlcNAc-(1→3)-β-D-Gal-(1→4)-β-D-Glc	Sialyllacto-N-tetraose d
HMO18	999.36	α-L-Fuc-(1→2)-β-D-Gal-(1→3)-[α-L-Fuc-(1→4)]-β-D-GlcNAc-(1→3)-β-D-Gal-(1→4)-β-D-Glc	Lacto-N-difucohexaose I
HMO19	999.36	β-D-Gal-(1→3)-[α-L-Fuc-(1→4)]-β-D-GlcNAc-(1→3)-β-D-Gal-(1→4)-[α-L-Fuc-(1→3)]-β-D-Glc	Lacto-N-difucohexaose II
HMO20	999.36	β-D-Gal-(1→4)-[α-L-Fuc-(1→3)]-β-D-GlcNAc-(1→3)-β-D-Gal-(1→4)-[α- L-Fuc-(1→3)]-β-D-Glc	Lacto-N-neodifucohexaose
HMO21	1072.38	β-D-Gal-(1→4)-β-D-GlcNAc-(1→3)-β-D-Gal-(1→4)-β-D-GlcNAc-(1→3)-β-D-Gal-(1→4)-β-D-Glc	Para Lacto-N-neohexaose
HMO22	1072.38	β-D-Gal-(1→4)-β-D-GlcNAc-(1→6)-[β-D-Gal-(1→4)-β-D-GlcNAc-(1→3)]-β-D-Gal-(1→4)-β-D-Glc	Lacto-N-neohexaose
HMO23	1144.40	α-D-Neu5Ac-(2→3)-β-D-Gal-(1→3)-[α-L-Fuc-(1→4)]-β-D-GlcNAc-(1→3)-β-D-Gal-(1→4)-β-D-Glc	Sialyl monofucosyllacto-N-tetraose
HMO24	1144.40	α-L-Fuc-(1→2)-β-D-Gal-(1→3)-[α-D-Neu5Ac-(2→6)]-β-D-GlcNAc-(1→3)-β-D-Gal-(1→4)-β-D-Glc	Sialyl-lacto-N-fucopentaose V
HMO25	1289.44	α-D-Neu5Ac-(2→3)-β-D-Gal-(1→3)-[α-D-Neu5Ac-(2→6)]-β-D-GlcNAc-(1→3)-β-D-Gal-(1→4)-β-D-Glc	Disialyllacto-N-tetraose
HMO26	1364.50	β-D-Gal-(1→4)-[α-L-Fuc-(1→3)]-β-D-GlcNAc-(1→6)-[α-L-Fuc-	Difucosyllacto-N-

		(1→2)-β-D-Gal-(1→3)-β-D-GlcNAc-(1→3)]-β-D-Gal-(1→4)-β-D-Glc	hexaose a
HMO27	1364.50	β-D-Gal-(1→3)-[α-L-Fuc-(1→4)]-β-D-GlcNAc-(1→3)-β-D-Gal-(1→4)-[α-L-Fuc-(1→3)]-β-D-GlcNAc-(1→3)-β-D-Gal-(1→4)-β-D-Glc	Difucosyl-para-lacto-N-hexaose
HMO28	1438.29	β-D-Gal-(1→4)-β-D-GlcNAc-(1→3)-β-D-Gal(1→4)-β-D-GlcNAc (1→3)-β-D-Gal(1→4)-β-D-GlcNAc(1→3)-β-D-Gal(1→4)-β-D-Glc	Lacto-N-neooctaose
HMO29	545.20	β-D-GlcNAc-(1→3)-β-D-Gal(1→4)-β-D-Glc	Lacto-N-triaose
HMO30	691.25	α-D-GalNAc-(1→3)-[α-L-Fuc-(1→2)]-β-D-Gal-(1→4)-β-D-Glc	Blood group A antigen tetraose type 5
HMO31	1056.39	α-D-GalNAc-(1→3)-[α-L-Fuc-(1→2)]-β-D-Gal-(1→3)-β-GlcNAc(1→3)-β-D-Gal(1→4)-β-D-Glc	Blood group A antigen hexaose type 1

Table S2. Association constants (K_a) measured by ESI-MS for binding of BabA to purified HMOs in 40 mM aqueous ammonium acetate solutions (pH 6.8, 25 °C).

HMO	K_a (M^{-1}) [a]
HMO1	$(3.4\pm0.6) \times 10^3$
HMO2	$(3.7\pm0.6) \times 10^3$
HMO3	$(1.2\pm0.3) \times 10^3$
HMO4	$(4.1\pm0.7) \times 10^3$
HMO6	$(2.9\pm0.9) \times 10^3$
HMO7	$(4.1\pm0.9) \times 10^3$
HMO9	$(8.1\pm1.6) \times 10^3$
HMO18	$(1.5\pm0.6) \times 10^4$

a. Uncertainties correspond to one standard deviation.

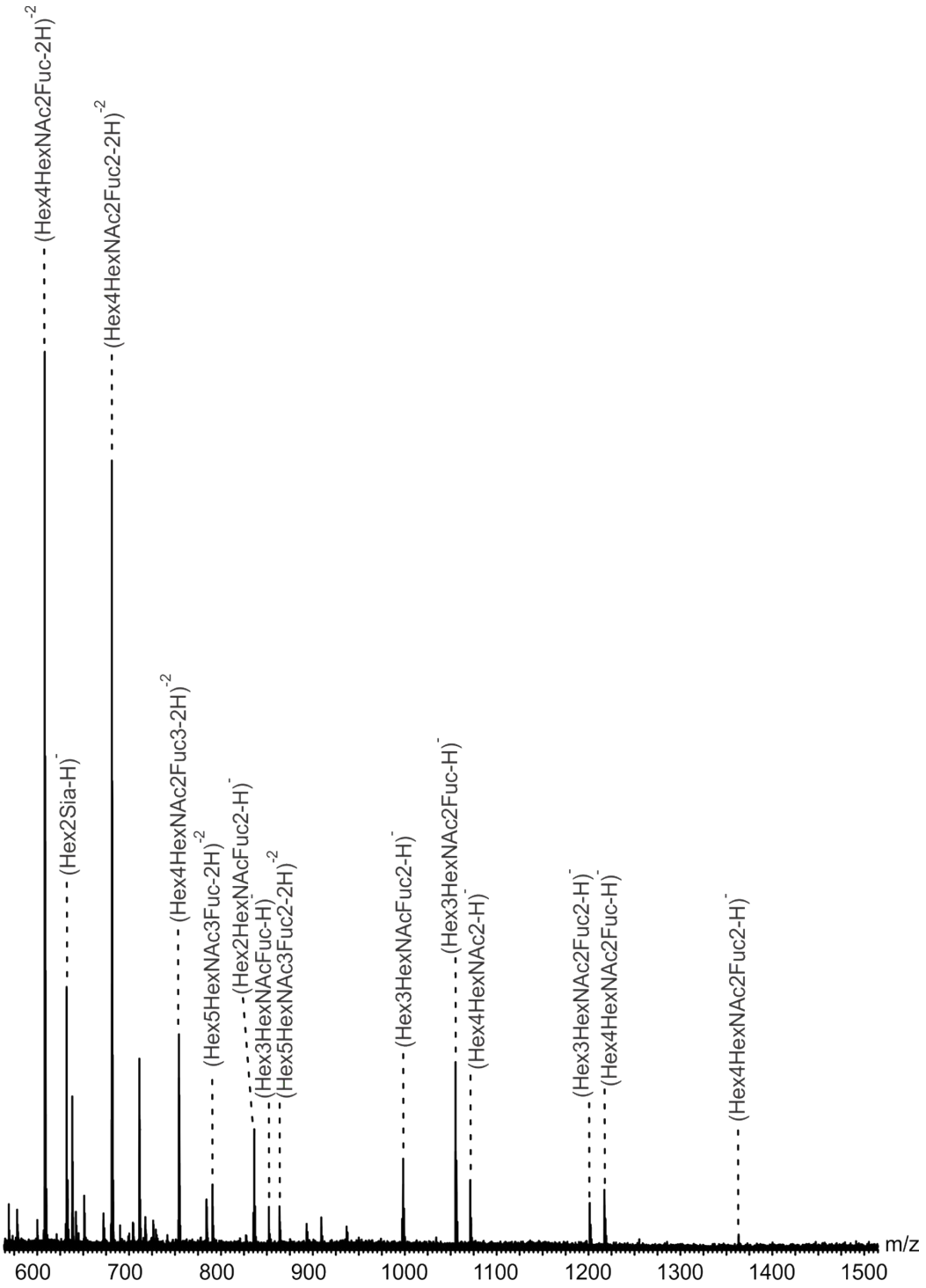

Figure S1. Representative ESI mass spectrum acquired in negative ion mode for an aqueous ammonium acetate solution (20 mM, pH 6.8) of *Fr1* (0.05 μg μL^{-1}).

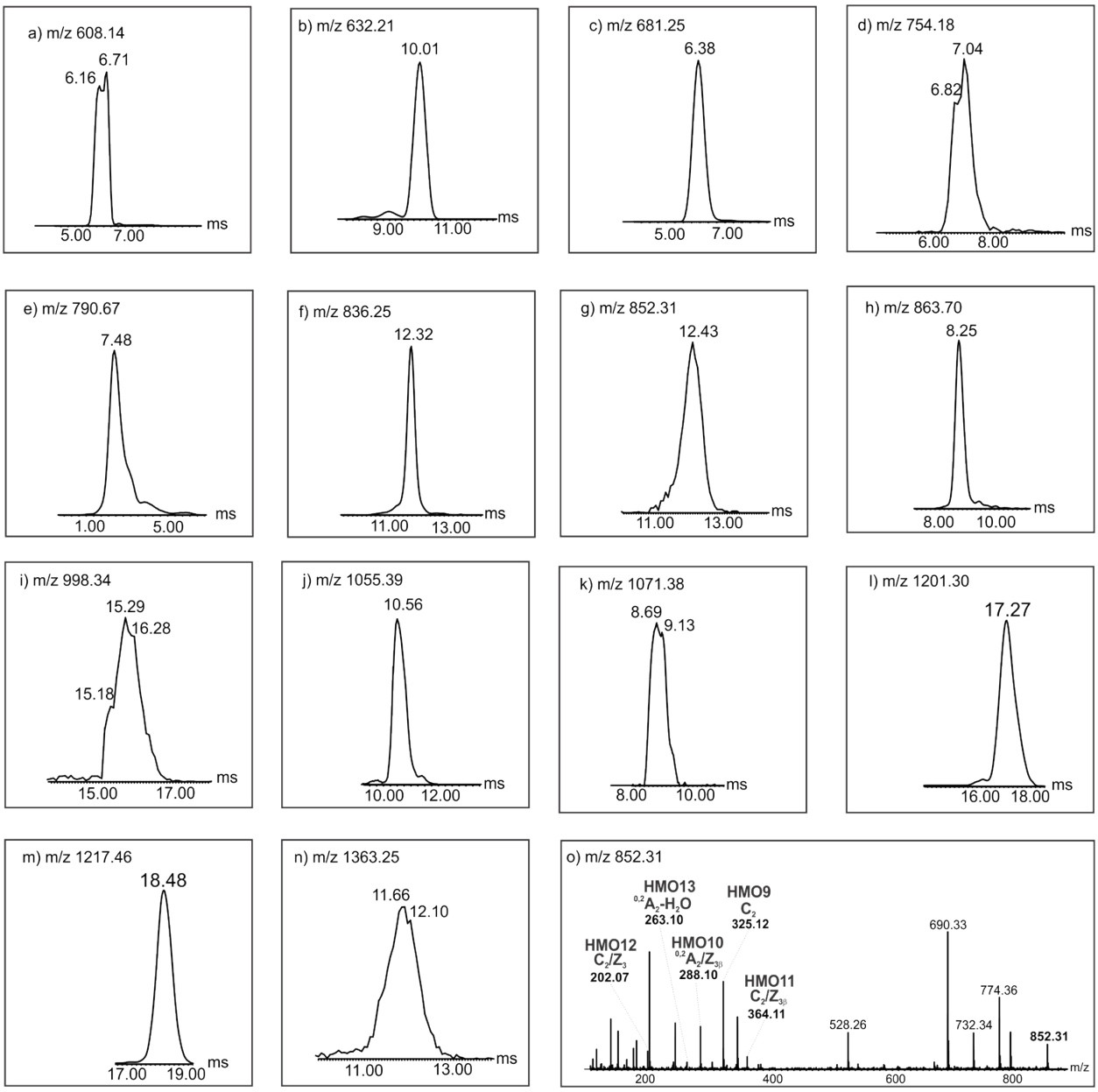

Figure S2; IMS-ATDs of deprotonated HMO ions produced from *Fr1*: (a) m/z 608.14; (b) m/z 632.21; (c) m/z 681.25; (d) m/z 754.18; (e) m/z 790.67; (f) m/z 836.25; (g) m/z 852.31; (h) m/z 863.70; (i) m/z 998.36; (j) m/z 1055.39; (k) m/z 1071.38; (l) m/z 1201.30; (m) m/z 1217.46 and (n) m/z 1363.25. (o) CID mass spectrum acquired in the Transfer region at 30 V for deprotonated HMO ions at m/z 852.31.

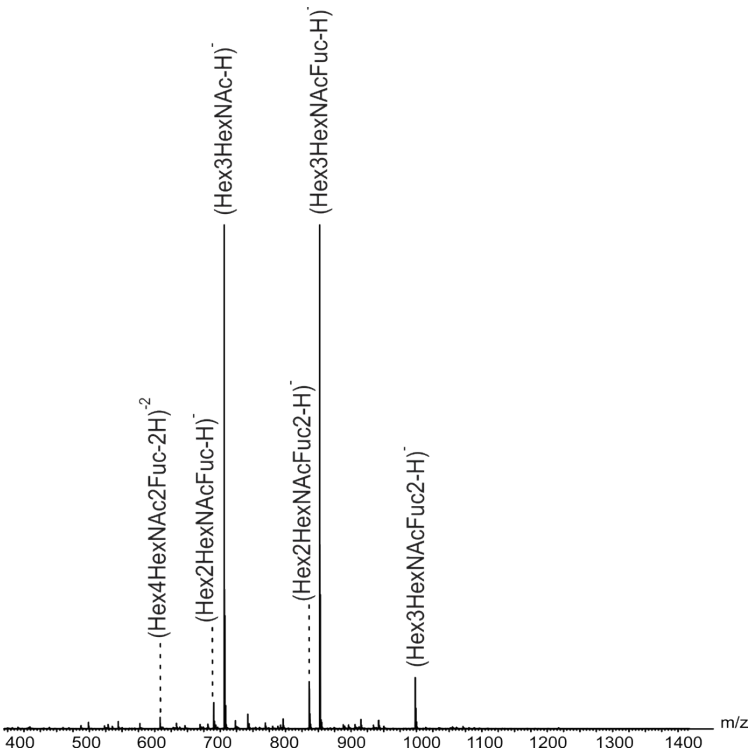

Figure S3. Representative ESI mass spectrum acquired in negative ion mode for an aqueous ammonium acetate solution (20 mM, pH 6.8) of *Fr2* (0.05 μg μL^{-1}).

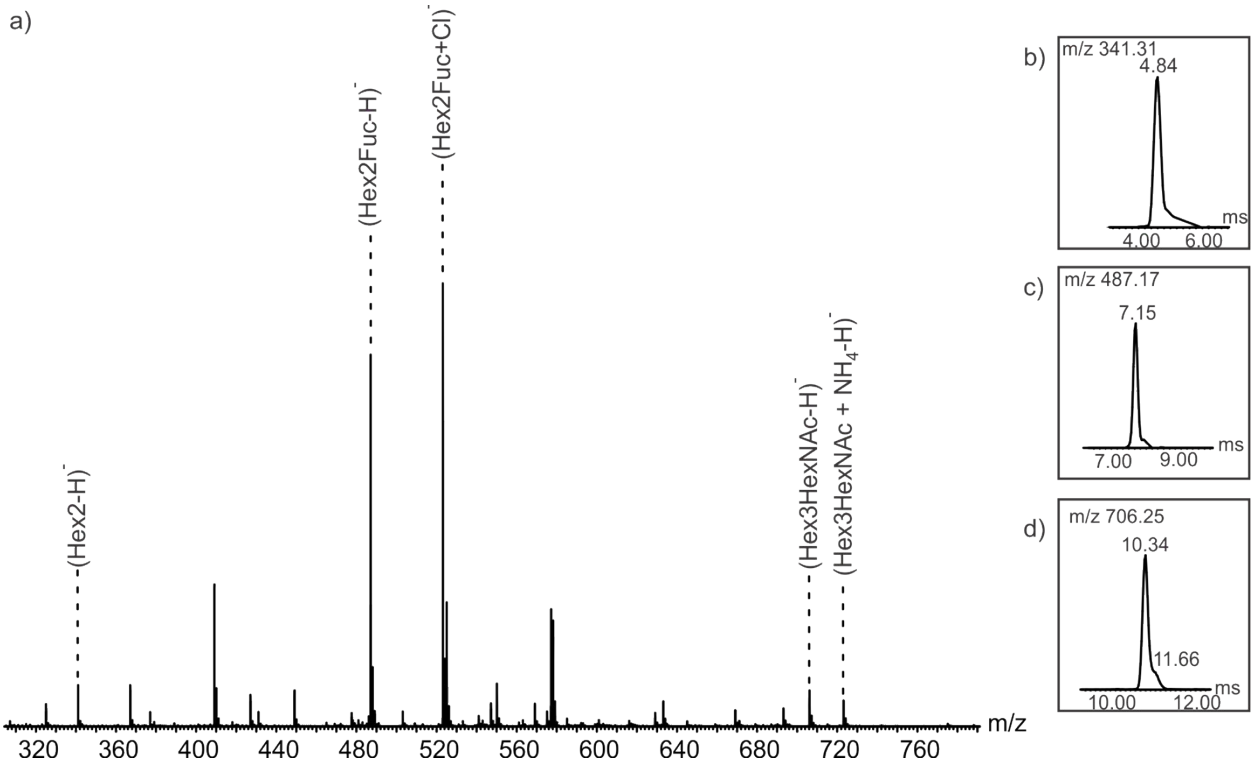

Figure S4 (a) Representative ESI mass spectrum acquired in negative ion mode for an aqueous ammonium acetate solution (20 mM, pH 6.8) of *Fr3* (0.05 μg μL^{-1}). IMS-ATDs measured for deprotonated HMO ions with (b) m/z 341.31, (c) m/z 487.17 and (d) m/z 706.25.

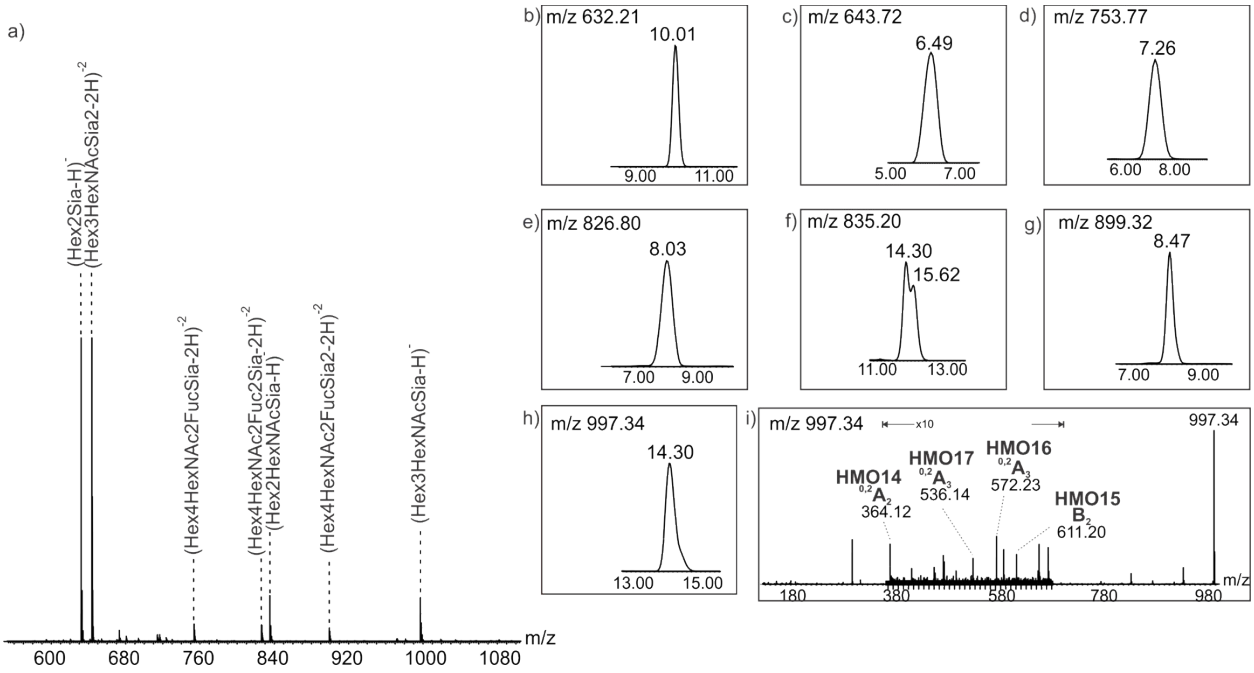

Figure S5 (a) Representative ESI mass spectrum acquired in negative ion mode for aqueous ammonium acetate solution (20 mM, pH 6.8) of *Fr4* (0.05 μg μL^{-1}). IMS-ATDs measured for deprotonated HMO ions with (b) m/z 632.21; (c) m/z 643.72; (d) m/z 753.77; (e) m/z 826.80; (f) m/z 835.20 and (g) m/z 899.32. (i) CID mass spectrum acquired in the Transfer region at 30 V for deprotonated HMO ions at m/z 997.34.

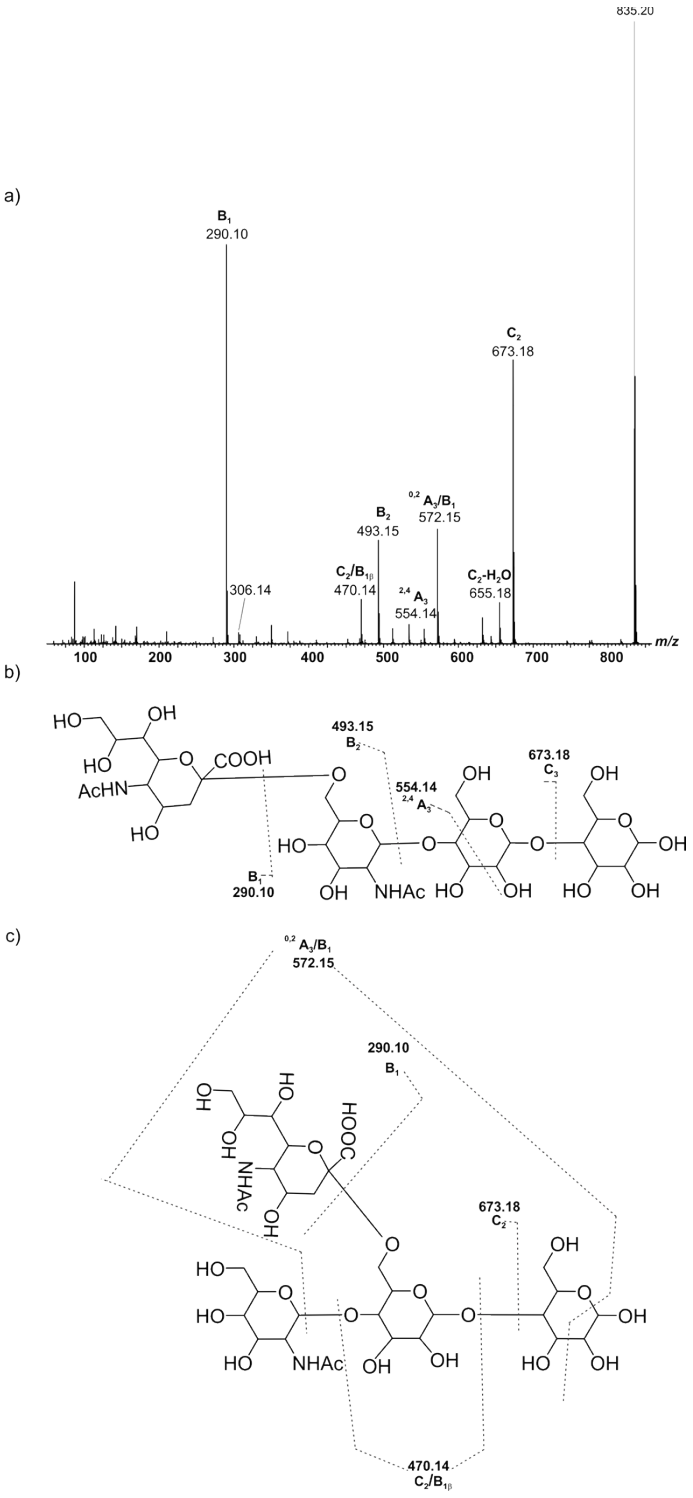

Figure S6. CID mass spectrum acquired for deprotonated HMO ions at m/z 835.20. Fragmentation scheme shown for (b) β- GlcNAc-(1→3)-[α-Neu5Ac-(2→6)]-β-Gal-(1→4)-β-Glc and (c) α-Neu5Ac-(2→6)-β-GlcNAc-(1→3/6)-β-Gal-(1→4)-β-Glc.

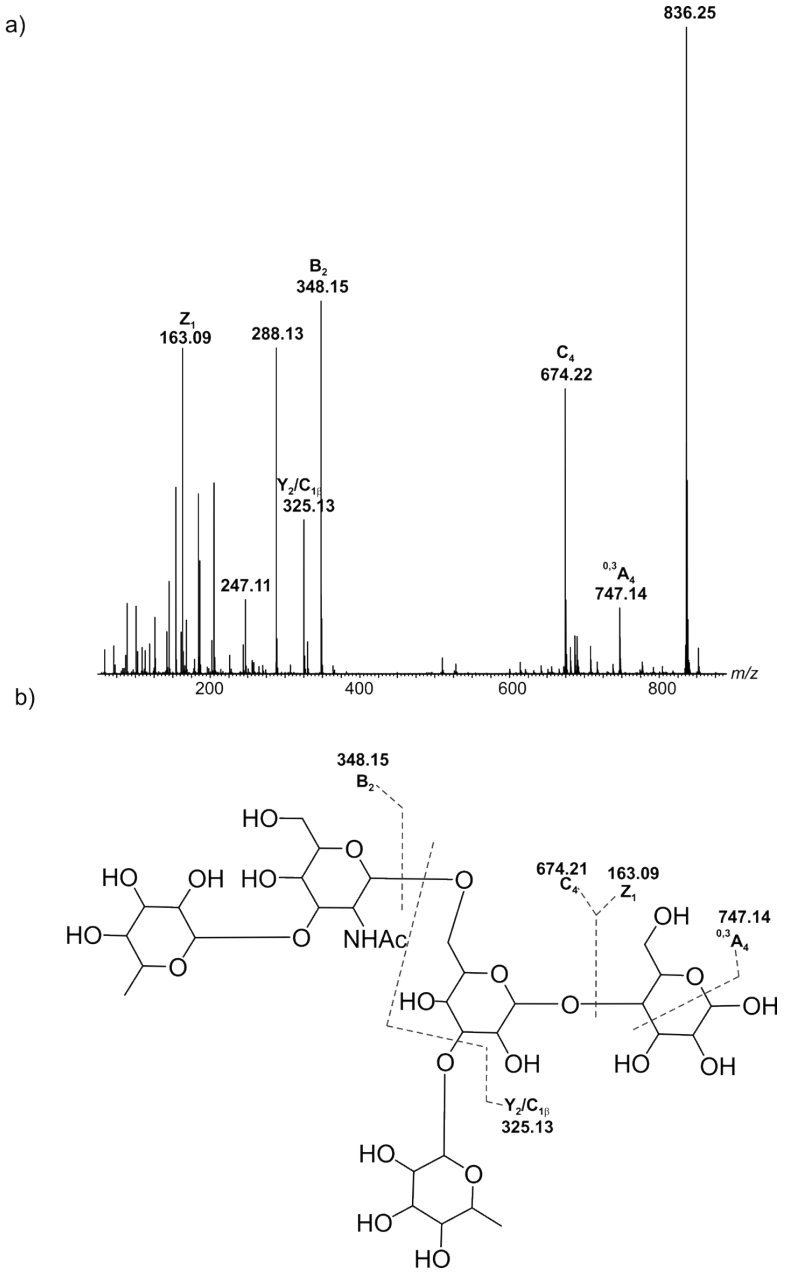

Figure S7. CID mass spectrum acquired for deprotonated HMO ions at m/z 836.25. (b) Fragmentation scheme shown for α-L-Fuc-(1→3)-β-D-GlcNAc-(1→6)-[α-L-Fuc-(1→3)]-β-D-Gal-(1→4)-β-D-Glc.

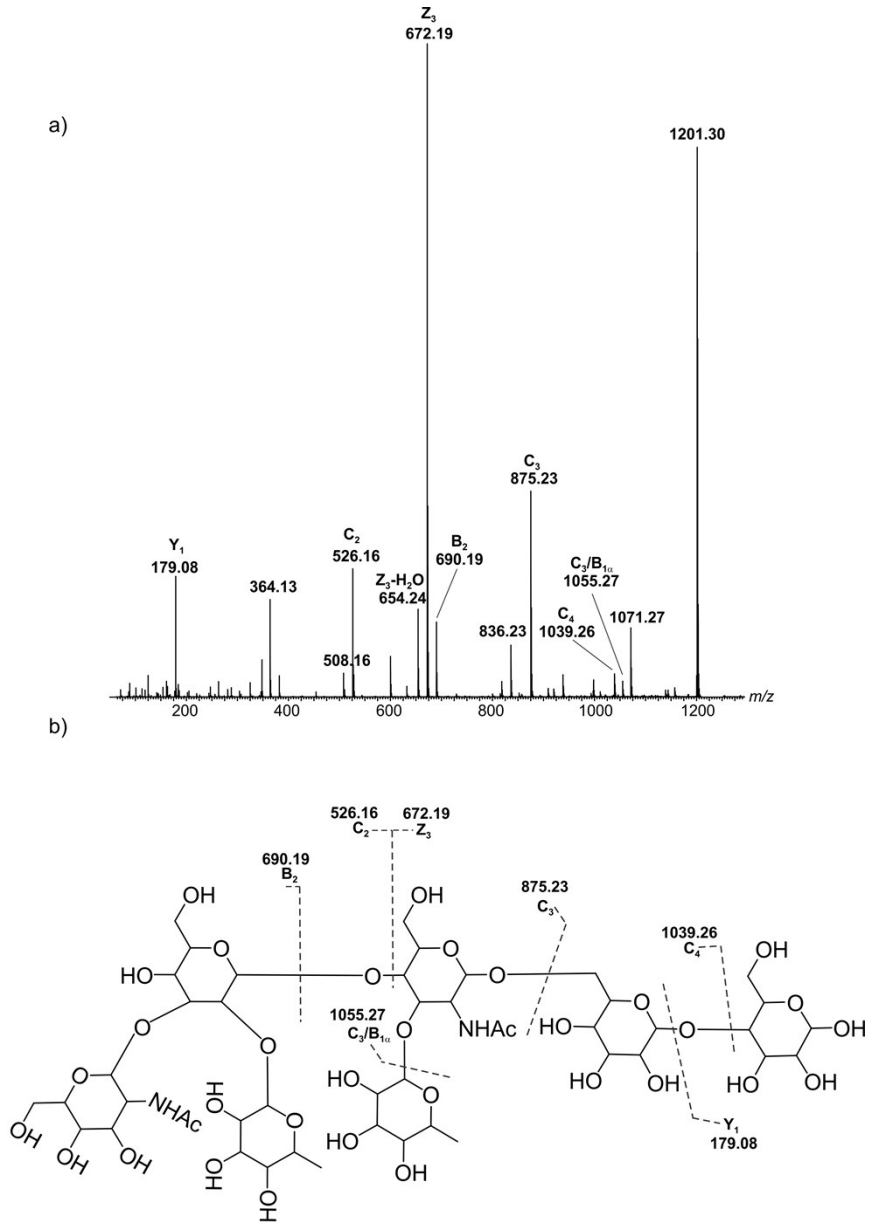

Figure S8. CID mass spectrum acquired for deprotonated HMO ions at m/z 1201.30. (b) Fragmentation scheme shown for β-D-GlcNAc-(1→3)-[L-Fuc-(1→3)]-β-D-Gal-(1→4)-[L-Fuc-(1→3)]-β-D-GlcNAc-(1→6)-β-D-Gal-(1→4)-β-D-Glc.

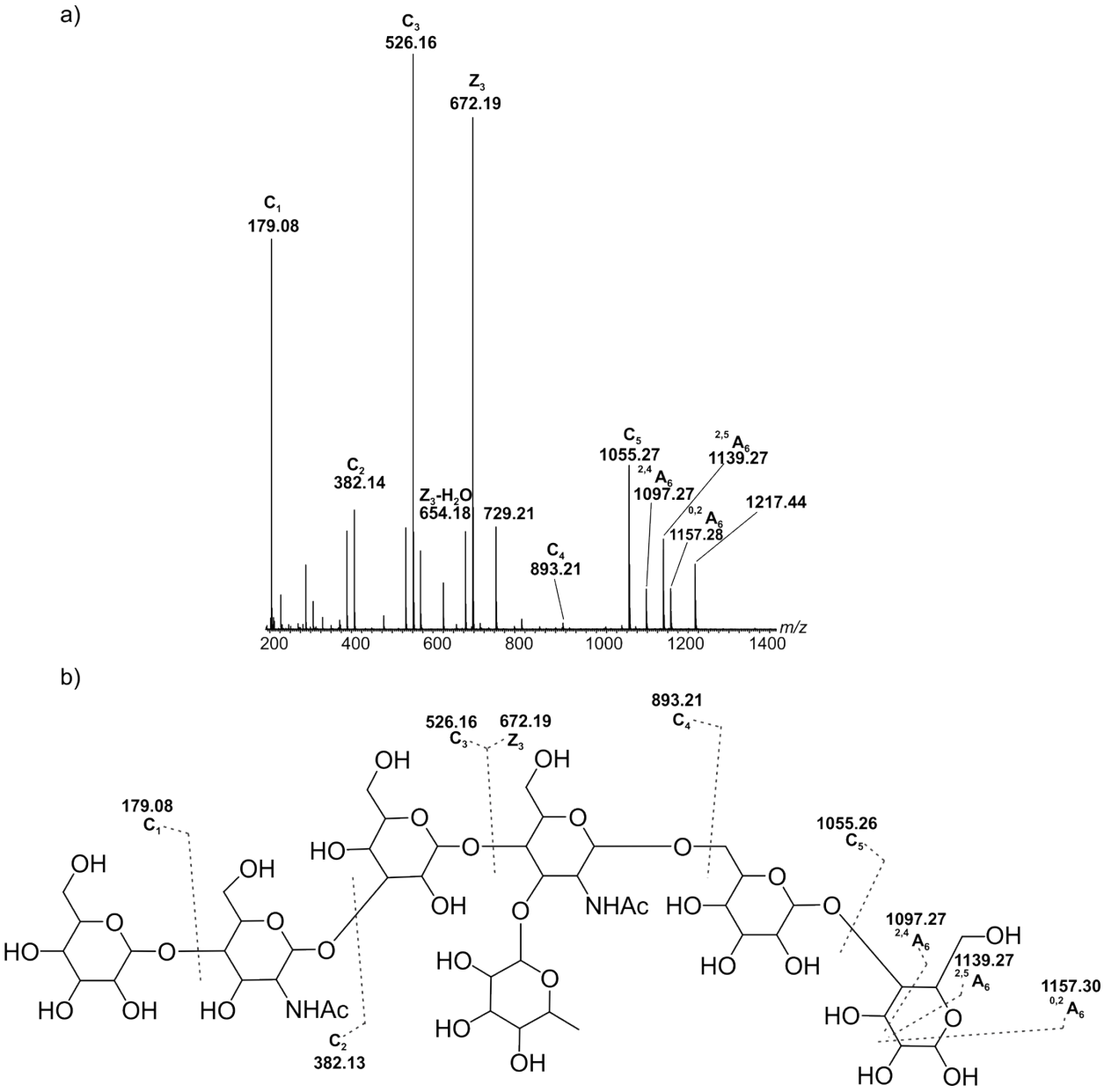

Figure S9. CID mass spectrum acquired for deprotonated HMO ions at m/z 1217.44. (b) Fragmentation scheme shown for β-D-Gal-(1→4)-β-D-GlcNAc-(1→3)-β-D-Gal-(1→4)-[L-Fuc-(1→3)]-β-D-GlcNAc-(1→6)-β-D-Gal-(1→4)-β-D-Glc.

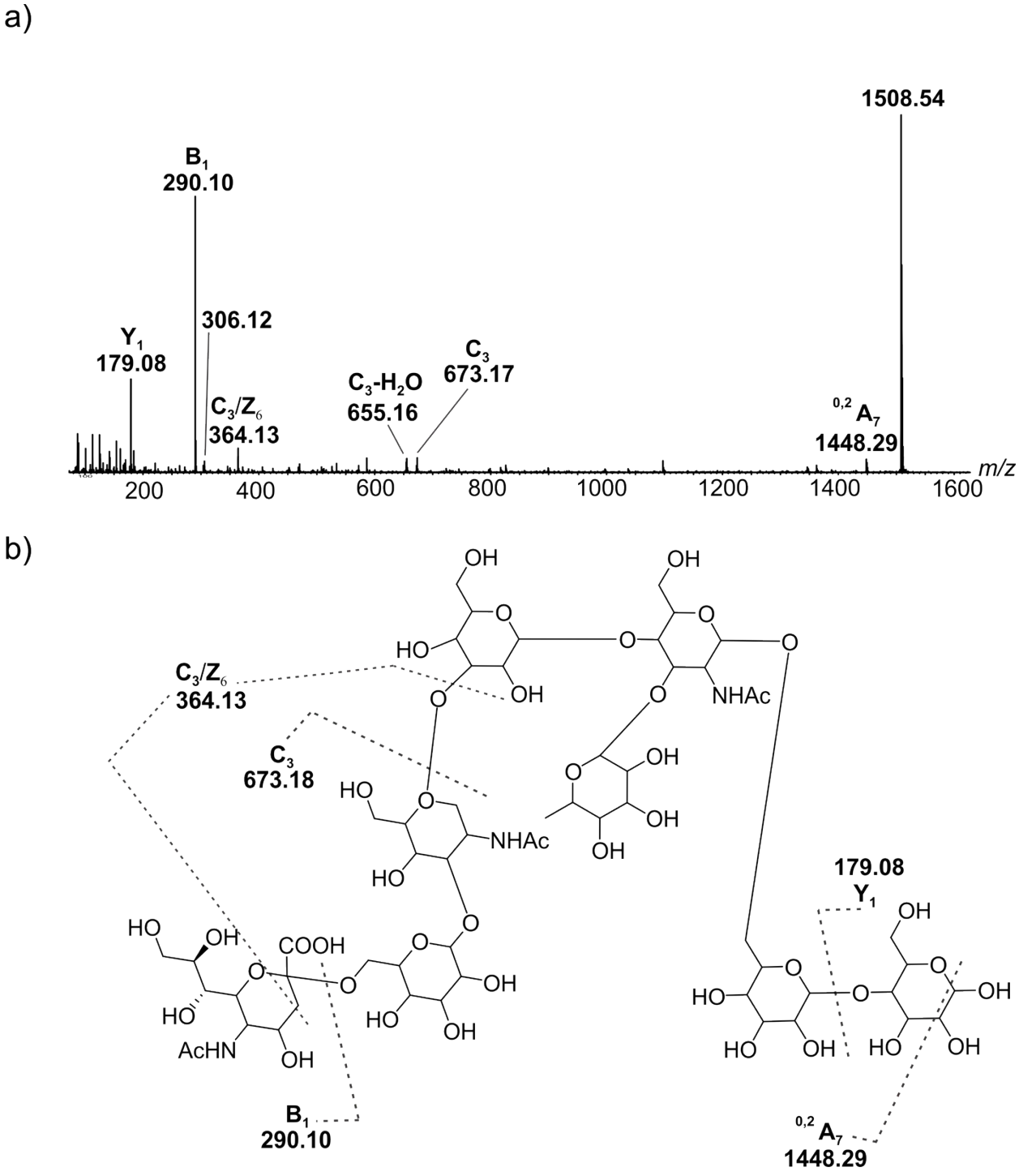

Figure S10. CID mass spectrum acquired for deprotonated HMO ions at m/z 1508.54. (b) Fragmentation scheme shown for α-D-Neu5Ac-(2→6)-β-D-Gal-(1→3)-β-D-GlcNAc-(1→3)-β-D-Gal-(1→4)-[L-Fuc-(1→3)]-β-D-GlcNAc-(1→6)-β-D-Gal-(1→4)-β-D-Glc.

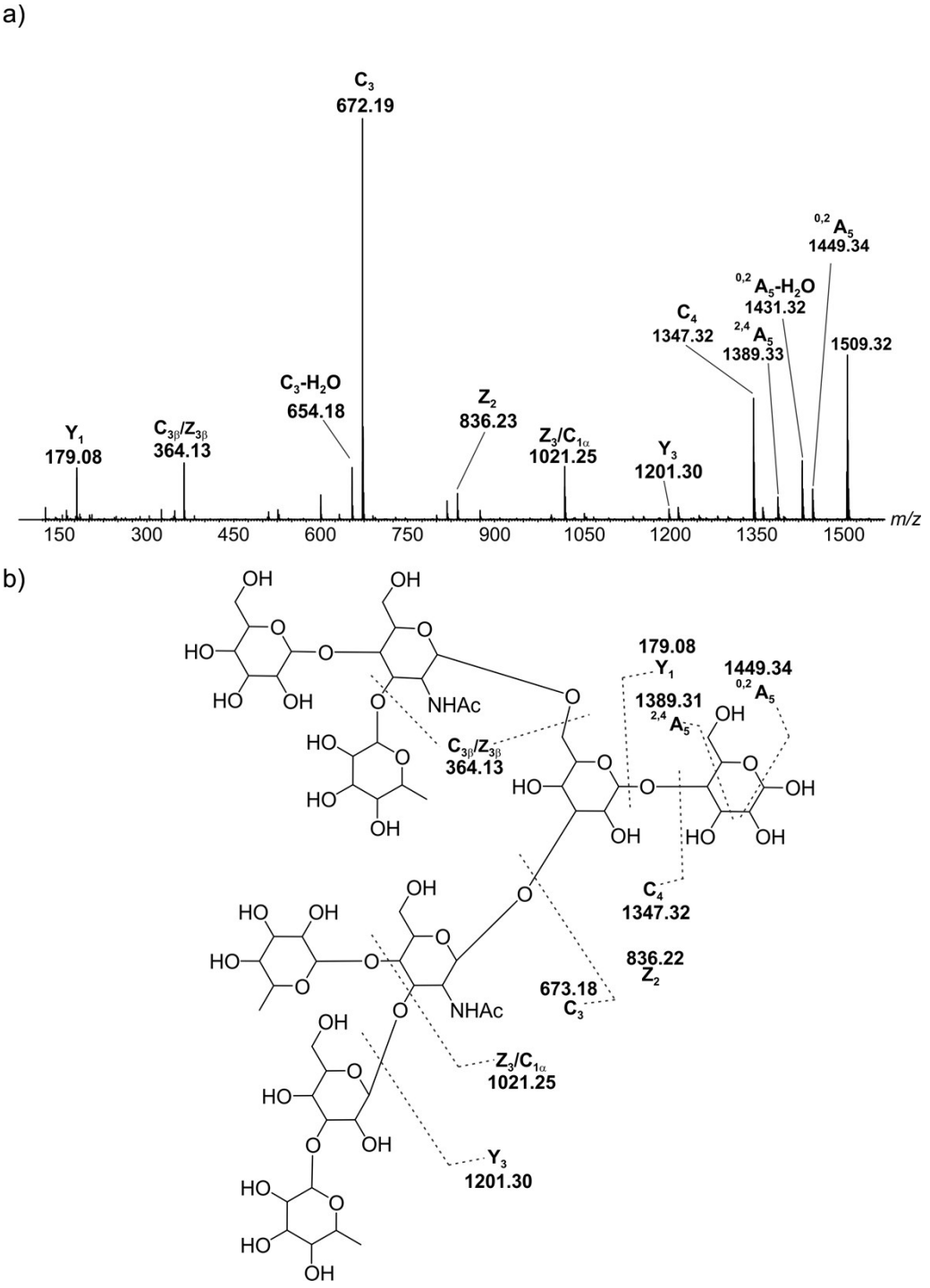

Figure S11. CID mass spectrum acquired for deprotonated HMO ions at m/z 1509.32. (b) Fragmentation scheme shown for α-L-Fuc-(1→3)-β-D-Gal-(1→3)-[α-L-Fuc-(1→4)]-β-D-GlcNAc-(1→3)-[β-D-Gal-(1→4)-[α-L-Fuc-(1→3)]-β-D-GlcNAc-(1→6)-]-β-D-Gal-(1→4)-β-D-Glc.

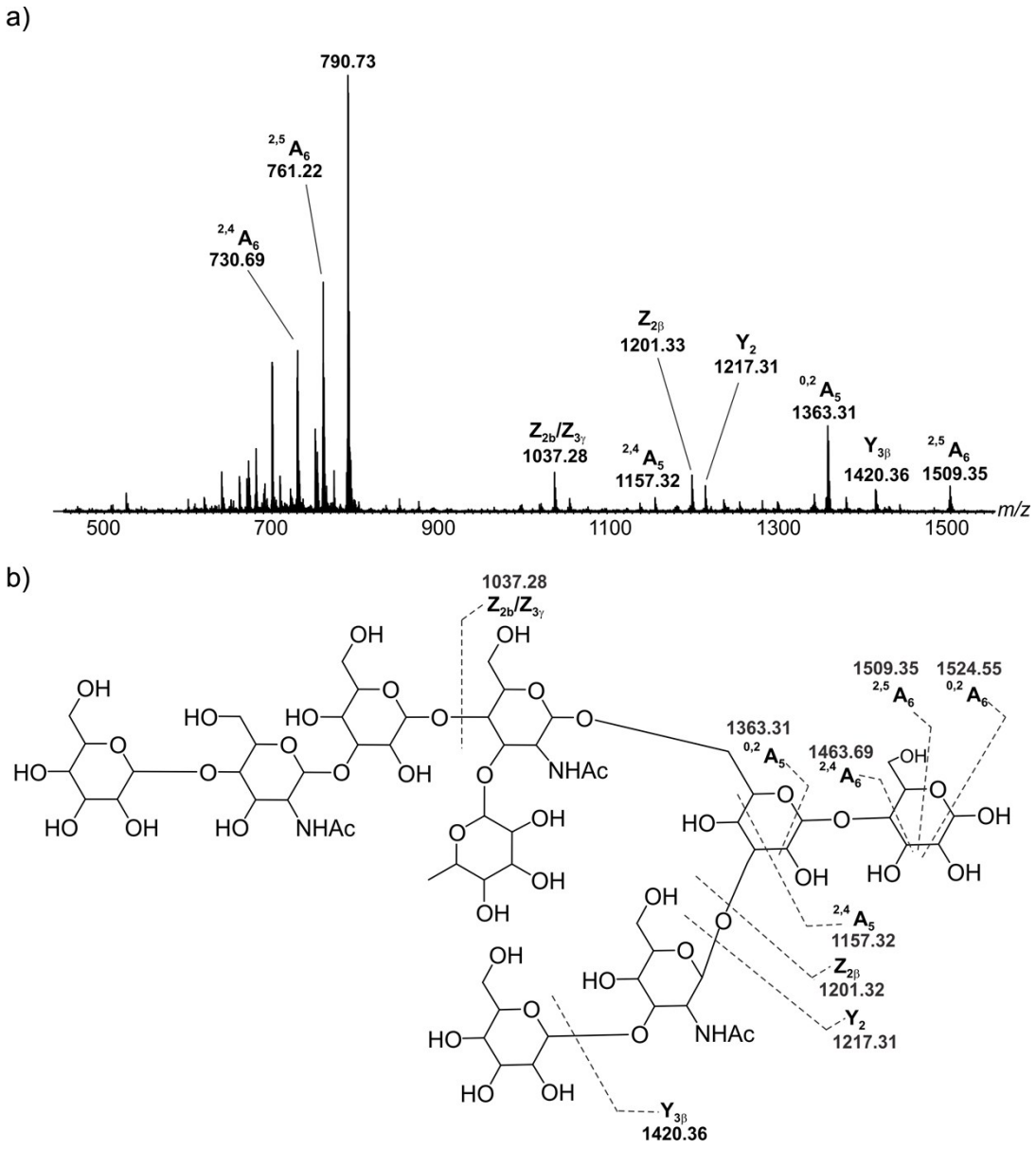

Figure S12. CID mass spectrum acquired for deprotonated HMO ions at m/z 790.73. (b) Fragmentation scheme shown for β-D-Gal-(1→4)-β-D-GlcNAc-(1→3)-β-D-Gal-(1→4)-[α-L-Fuc-(1→3)]-β-D-GlcNAc-(1→6)-[β-D-Gal-(1→4)-β-D-GlcNAc-(1→3)-]-β-D-Gal-(1→4)-β-D-Glc.

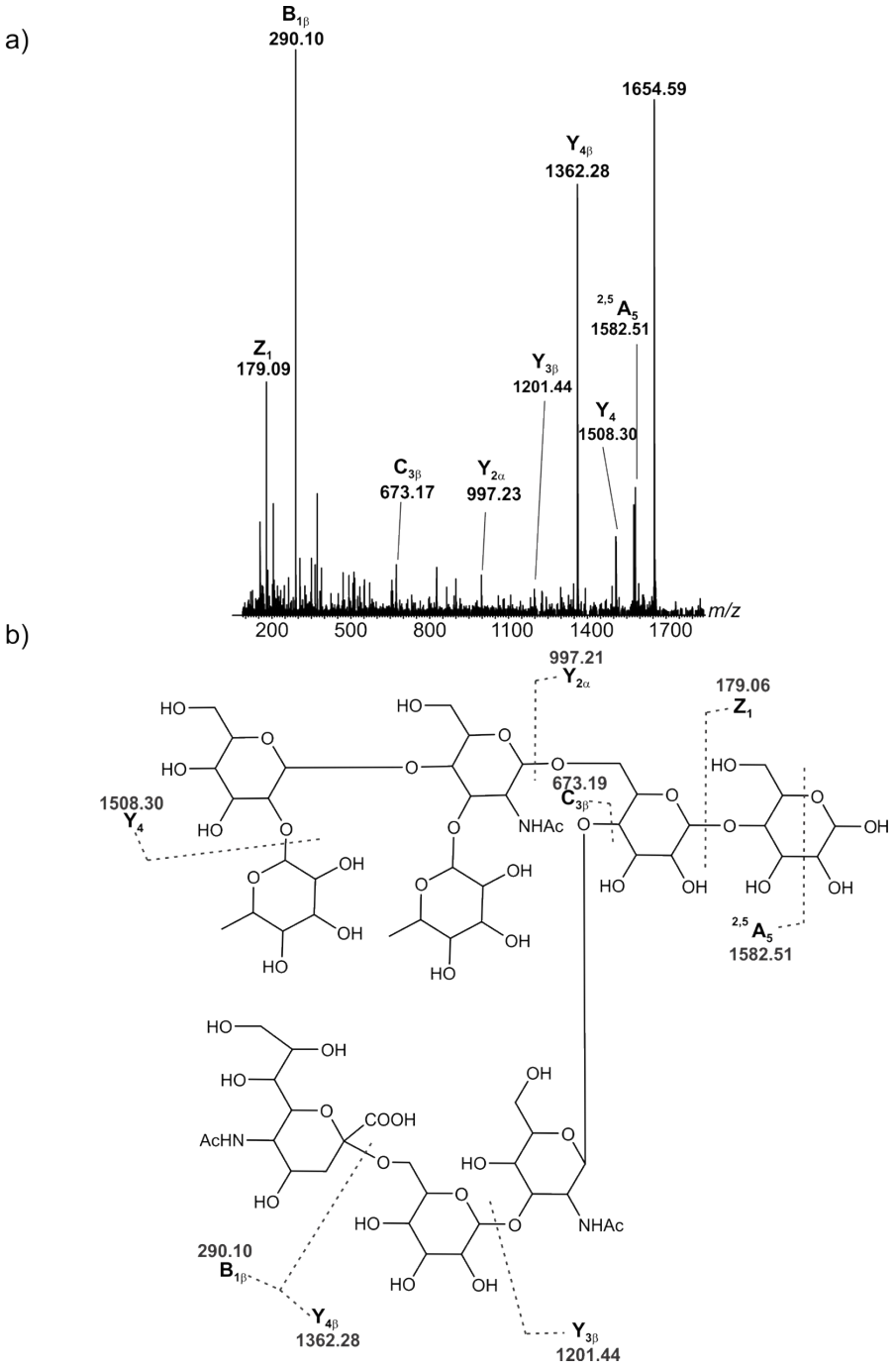

Figure S13. CID mass spectrum acquired for deprotonated HMO ions at m/z 1654.59. (b) Fragmentation scheme shown for L-Fuc-(1→2)-β-D-Gal-(1→4)-[α-L-Fuc-(1→3)-]-β-D-GlcNAc-(1→6)-[α-D-Neu5Ac-(2→6)-β-D-Gal-(1→3)-β-D-GlcNAc-(1→4)-]-β-D-Gal-(1→4)-β-D-Glc.

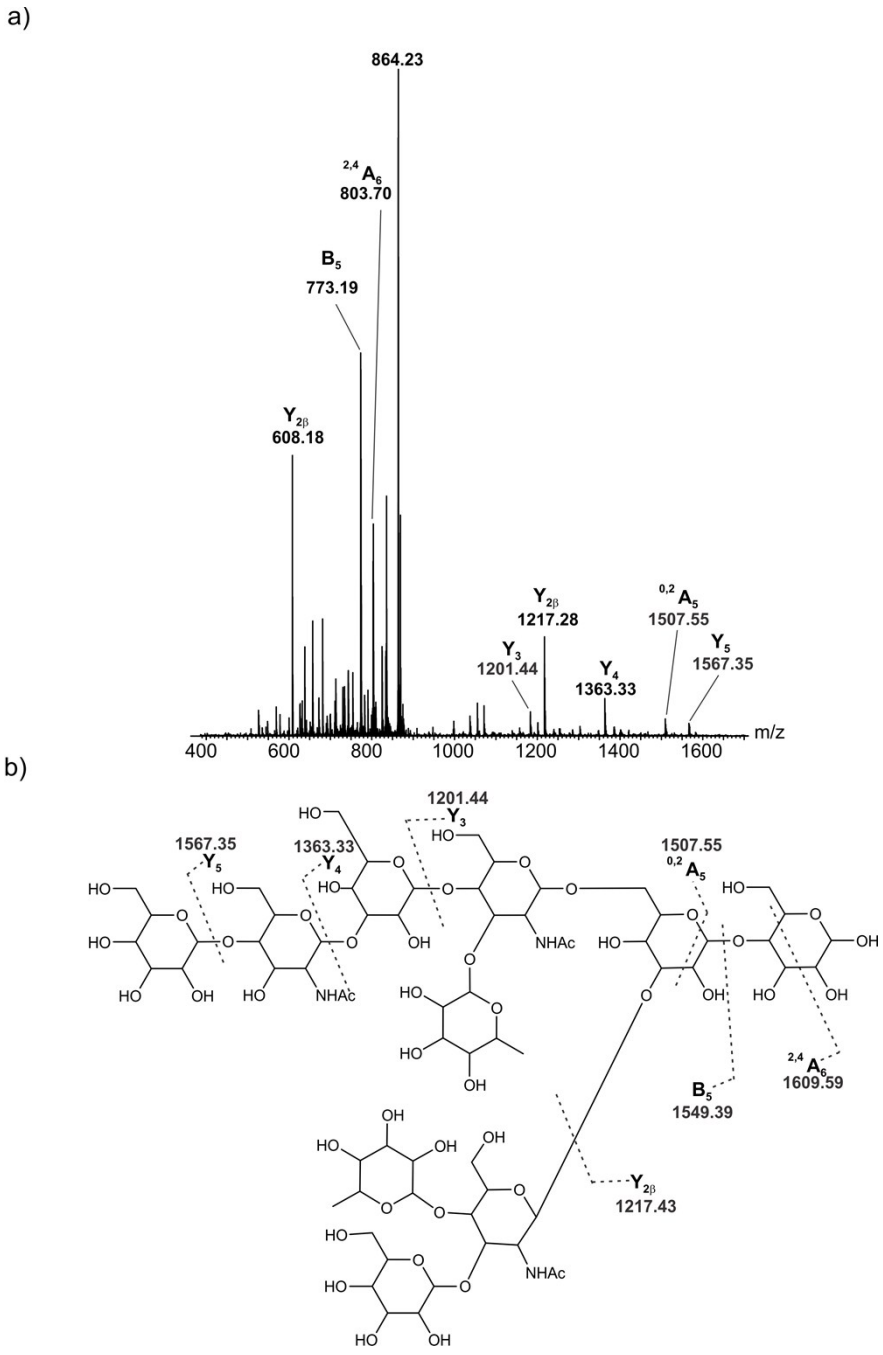

Figure S14. CID mass spectrum acquired for deprotonated HMO ions at m/z 864.23. (b) Fragmentation scheme shown for β-D-Gal-(1→4)-β-D-GlcNAc-(1→3)-β-D-Gal-(1→4)-[α-L-Fuc-(1→3)]-β-D-GlcNAc-(1→6)-[β-D-Gal-(1→3)-[α-L-Fuc-(1→4)-]-β-D-GlcNAc-(1→3)-]-β-D-Gal-(1→4)-β-D-Glc.

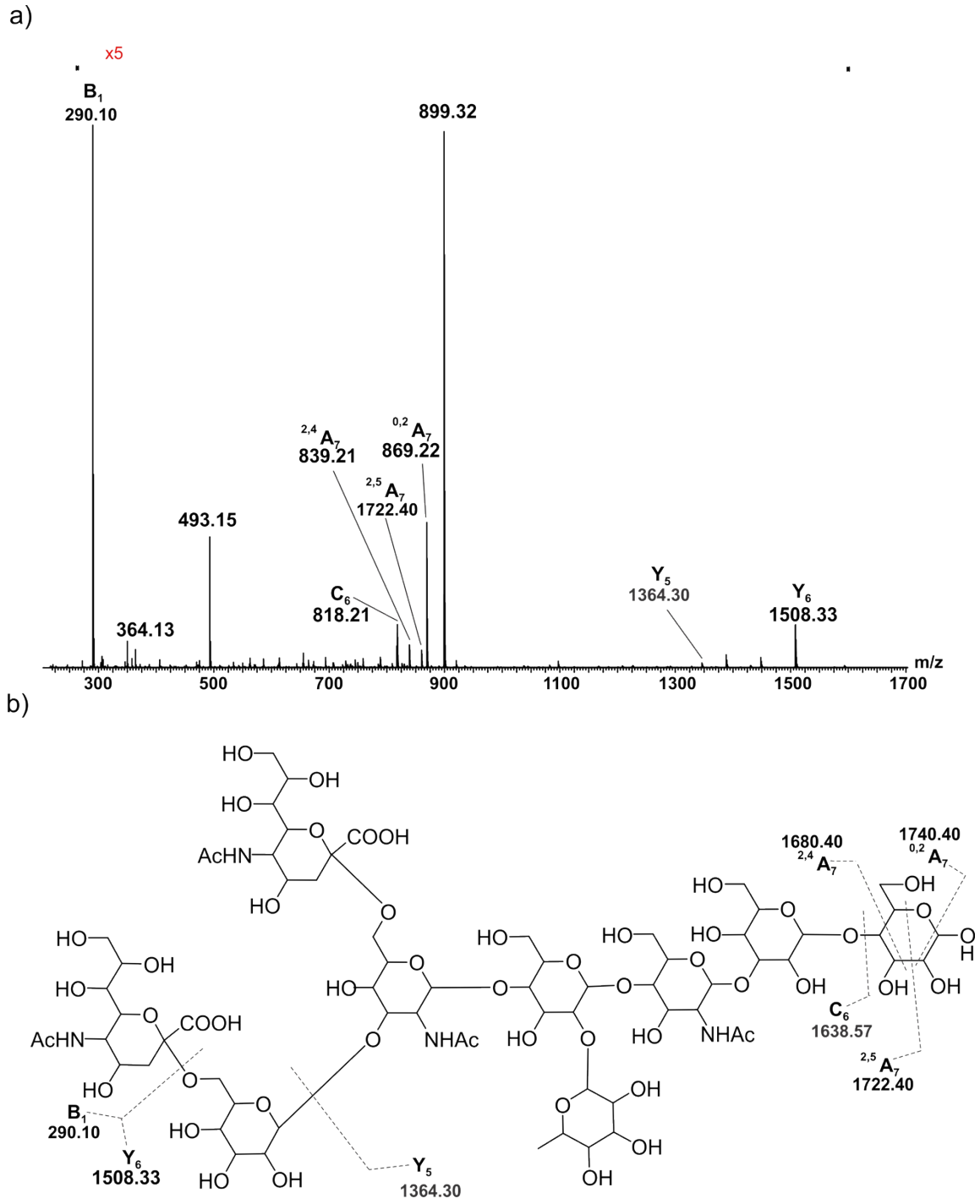

Figure S15. CID mass spectrum acquired for deprotonated HMO ions at m/z 899.32. (b) Fragmentation scheme shown for α-D-Neu5Ac-(2→6)-β-D-Gal-(1→4)-[α-D-Neu5Ac-(2→6)-]-β-D-GlcNAc-(1→4)-[L-Fuc-(1→2)]-β-D-Gal-(1→4)-β-D-GlcNAc-(1→3)-β-D-Gal-(1→4)-β-D-Glc.

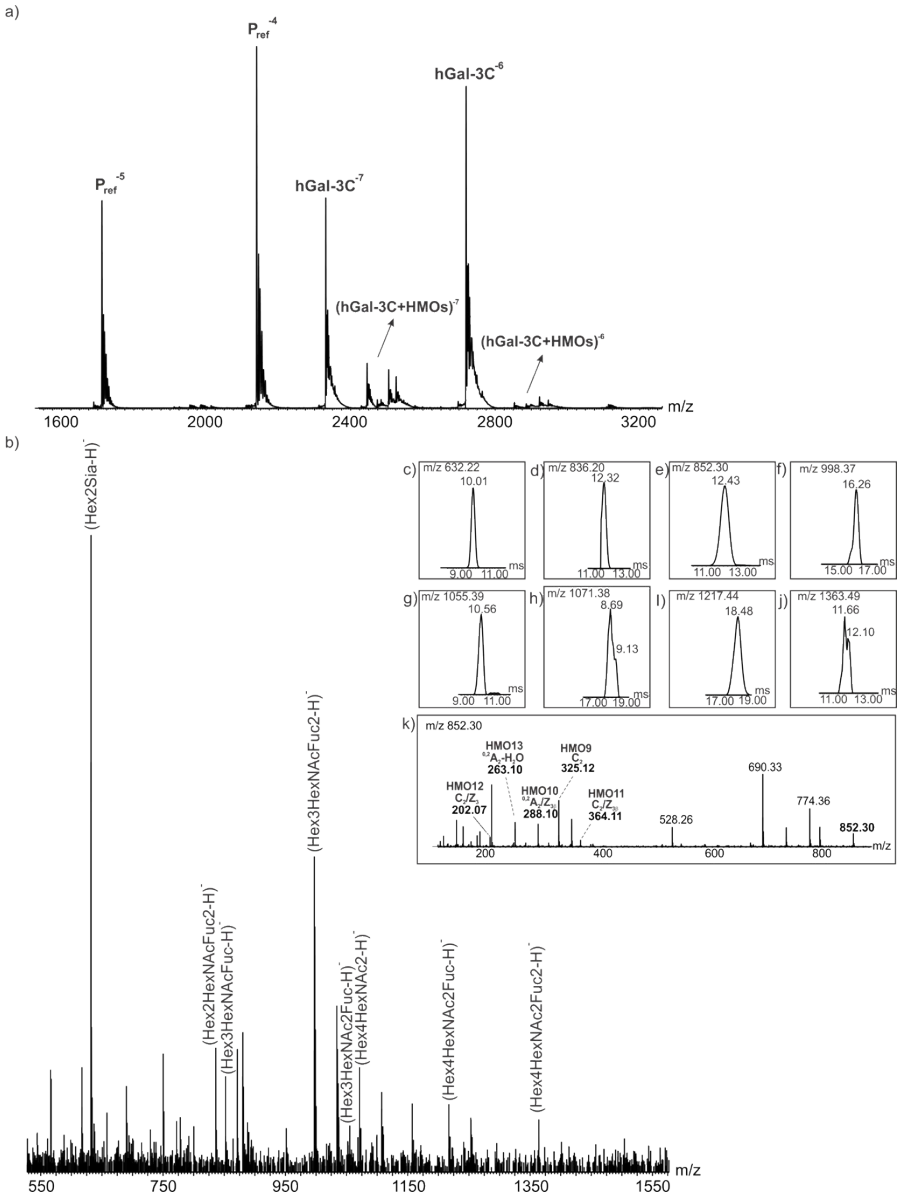

Figure S16. (a) Representative ESI mass spectrum acquired in negative ion mode for an aqueous ammonium acetate solution (20 mM, pH 6.8) of P_{ref} (5 μM), *Fr1* (0.05 μg μL^{-1}) and hGal-3C (15 μM). (b) CID mass spectrum acquired for all (hGal-3C + HMO)$^{7-}$ ions at Trap voltage 40 V. IMS-ATDs of released HMO ions at (c) m/z 632.22, (d) m/z 836.20, (e) m/z 852.30, (f) m/z 998.37, (g) m/z 1055.39, (h) m/z 1071.38, (i) m/z 1217.44 and (j) m/z 1363.49. (k) CID mass spectrum acquired in the Transfer region at 30 V for deprotonated HMO ions at m/z 852.30.

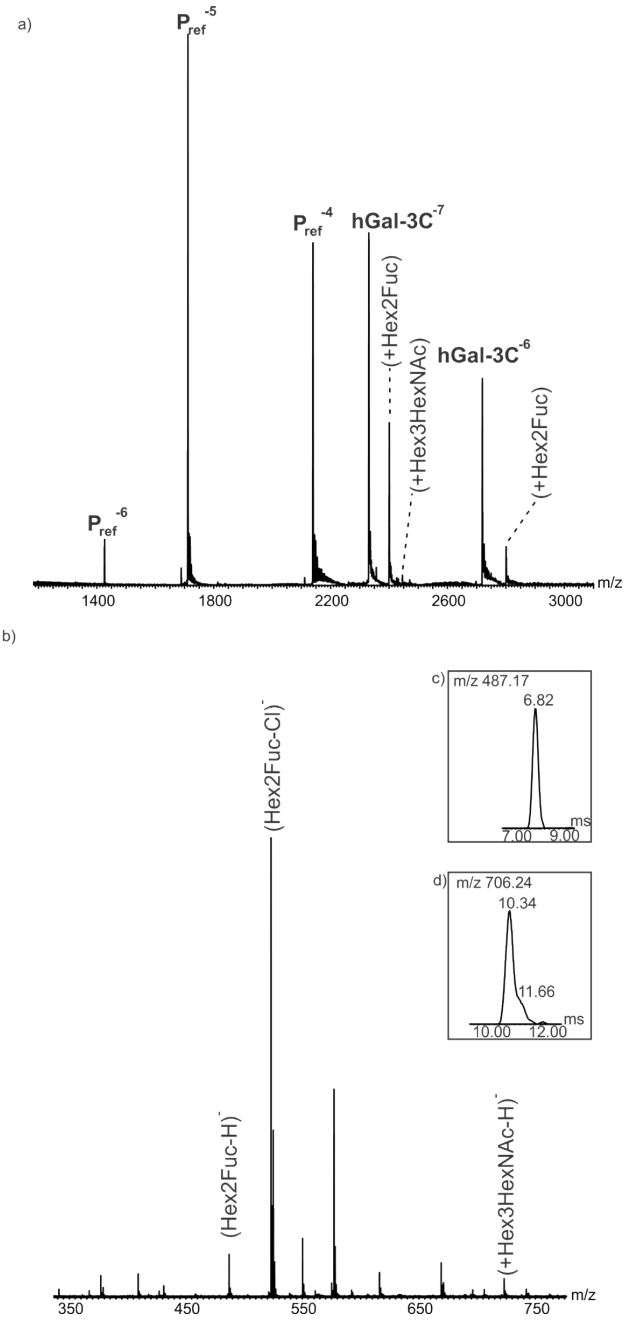

Figure S17. (a) Representative ESI mass spectrum acquired in negative ion mode for aqueous ammonium acetate solution (20 mM, pH 6.8) of P_{ref} (5 µM), *Fr3* (0.05 µg µL^{-1}) and hGal-3C (15 µM), (b) CID mass spectrum acquired for all (hGal-3C + HMO)$^{7-}$ ions at Trap voltage 40 V. IMS-ATDs of released HMO ions at (c) m/z 487.17 and (d) m/z 706.24.

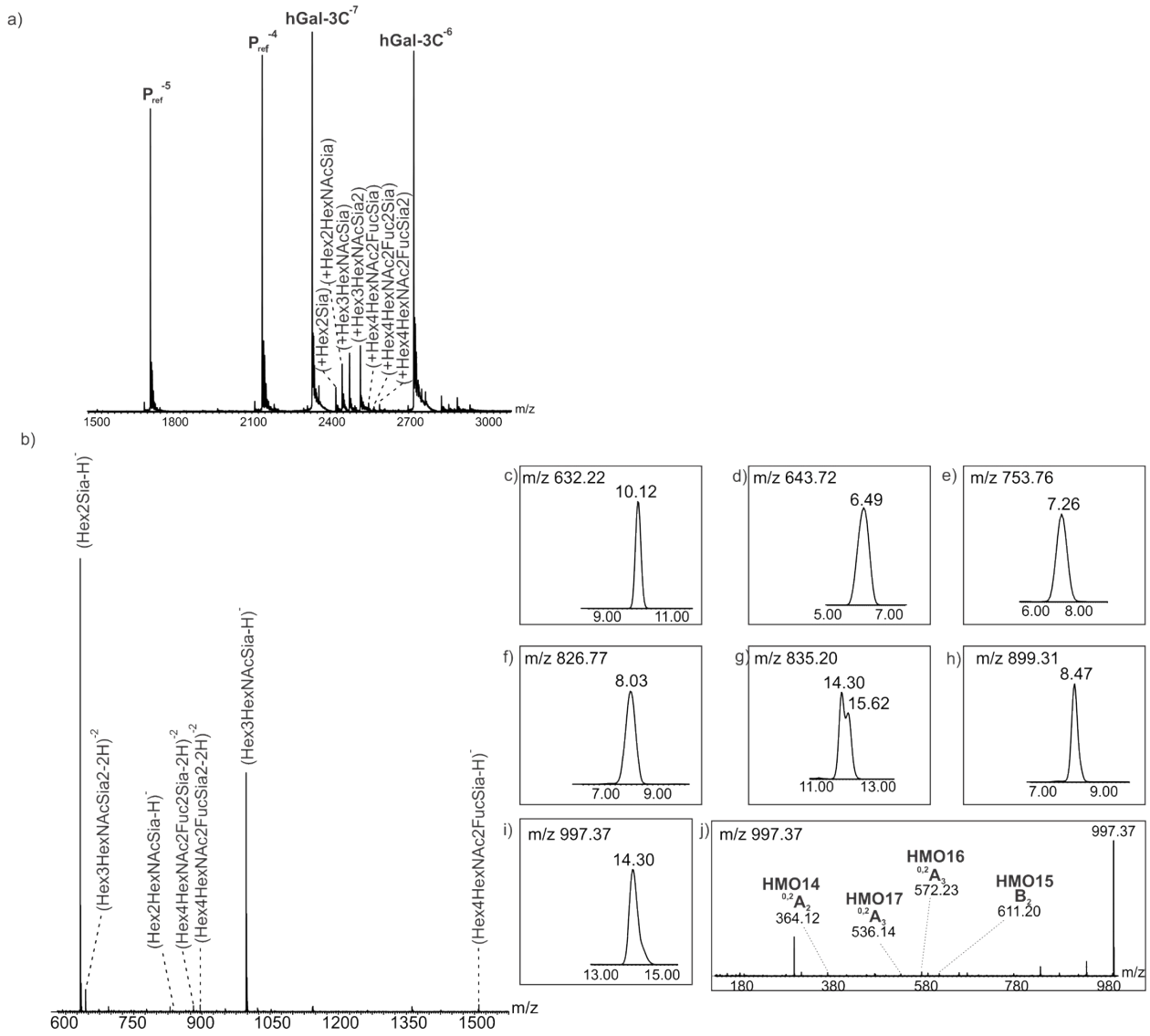

Figure S18. (a) Representative ESI mass spectrum acquired in negative ion mode for aqueous ammonium acetate solution (20 mM, pH 6.8) of P_{ref} (5 µM), *Fr4* (0.05 µg µL^{-1}) and hGal-3C (15 µM). (b) CID mass spectrum acquired for all (hGal-3C + HMO)$^{7-}$ ions at Trap voltage 40 V. IMS-ATDs of released HMO ions at (c) m/z 632.22, (d) m/z 643.72, (e) m/z 753.76, (f) m/z 826.77, (g) m/z 835.20, (h) m/z 899.31 and (i) m/z 997.37. (i) CID mass spectrum acquired in the Transfer region at 30 V for deprotonated HMO ions at m/z 997.37.

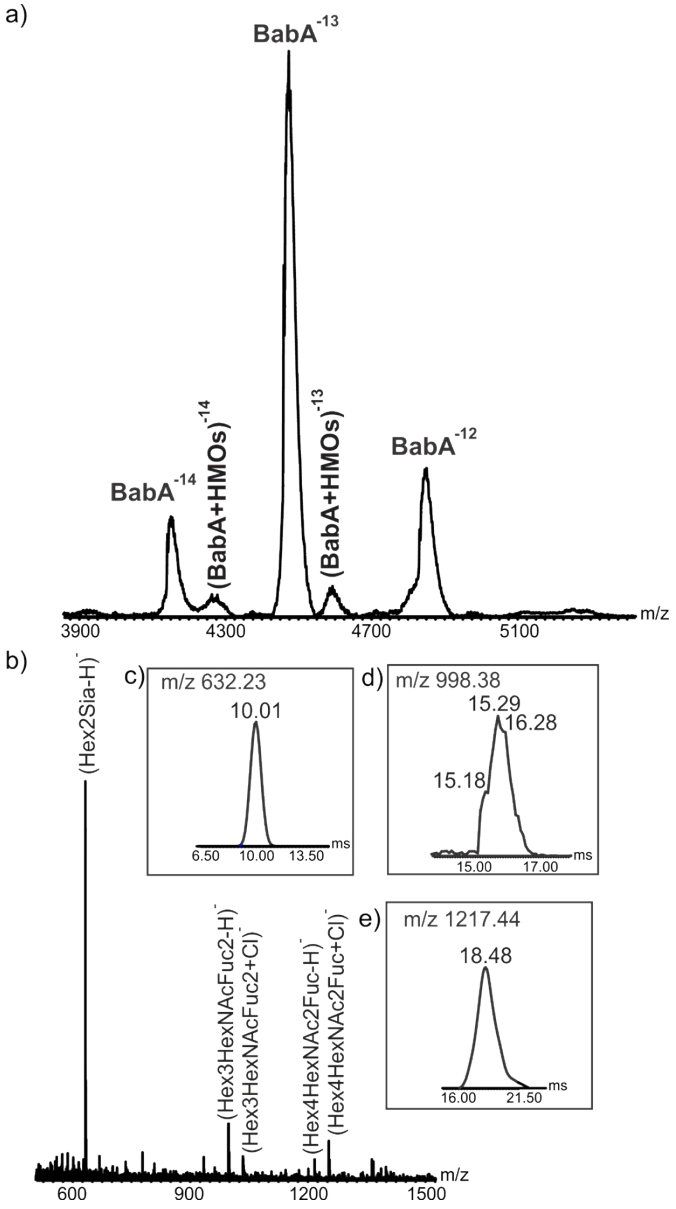

Figure S19. (a) Representative ESI mass spectrum acquired in negative ion mode for aqueous ammonium acetate solution (20 mM, pH 6.8) of *Fr1* (0.05 μg μL^{-1}) and BabA (5 μM). (b) CID mass spectrum acquired for all $(BabA + HMO)^{13-}$ ions at Trap voltage 90 V. IMS-ATDs of released HMO ions at (c) m/z 632.23, (d) m/z 998.38 and (e) m/z 1217.44.

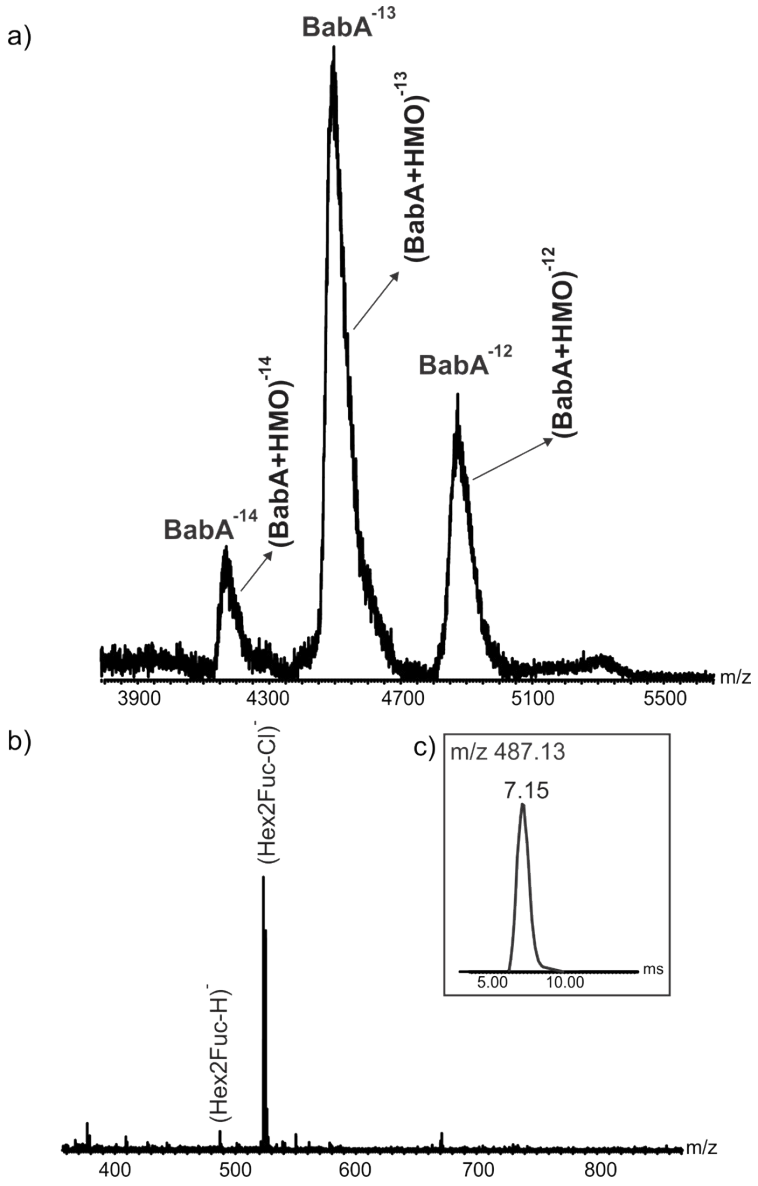

Figure S20. (a) Representative ESI mass spectrum acquired in negative ion mode for aqueous ammonium acetate solution (20 mM, pH 6.8) of *Fr3* (0.05 μg μL^{-1}) and BabA (5 μM). (b) CID mass spectrum acquired for all (BabA + HMO)$^{13-}$ ions at Trap voltage 90 V. (c) IMS-ATD of released HMO ions at m/z 487.13.

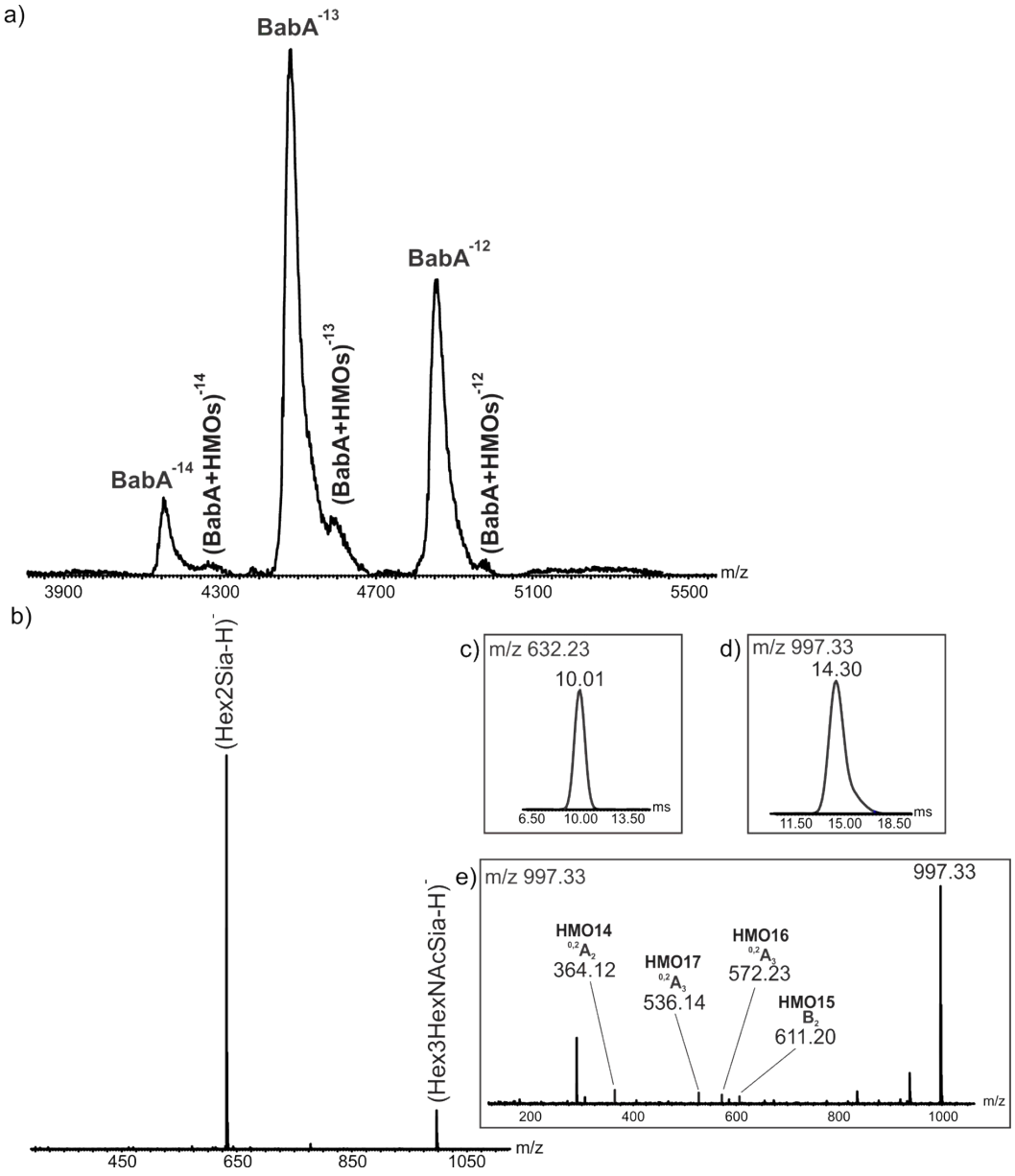

Figure S21. (a) Representative ESI mass spectrum acquired in negative ion mode for aqueous ammonium acetate solution (20 mM, pH 6.8) of *Fr4* (0.05 μg μL^{-1}) and BabA (5 μM). (b) CID mass spectrum acquired for all (BabA + HMO)$^{13-}$ ions at Trap voltage 90 V. IMS-ATDs of released HMO ions (c) m/z 632.23 and (d) m/z 997.33. (e) CID mass spectrum acquired in the Transfer region at 30 V for deprotonated HMO ions at m/z 997.33.

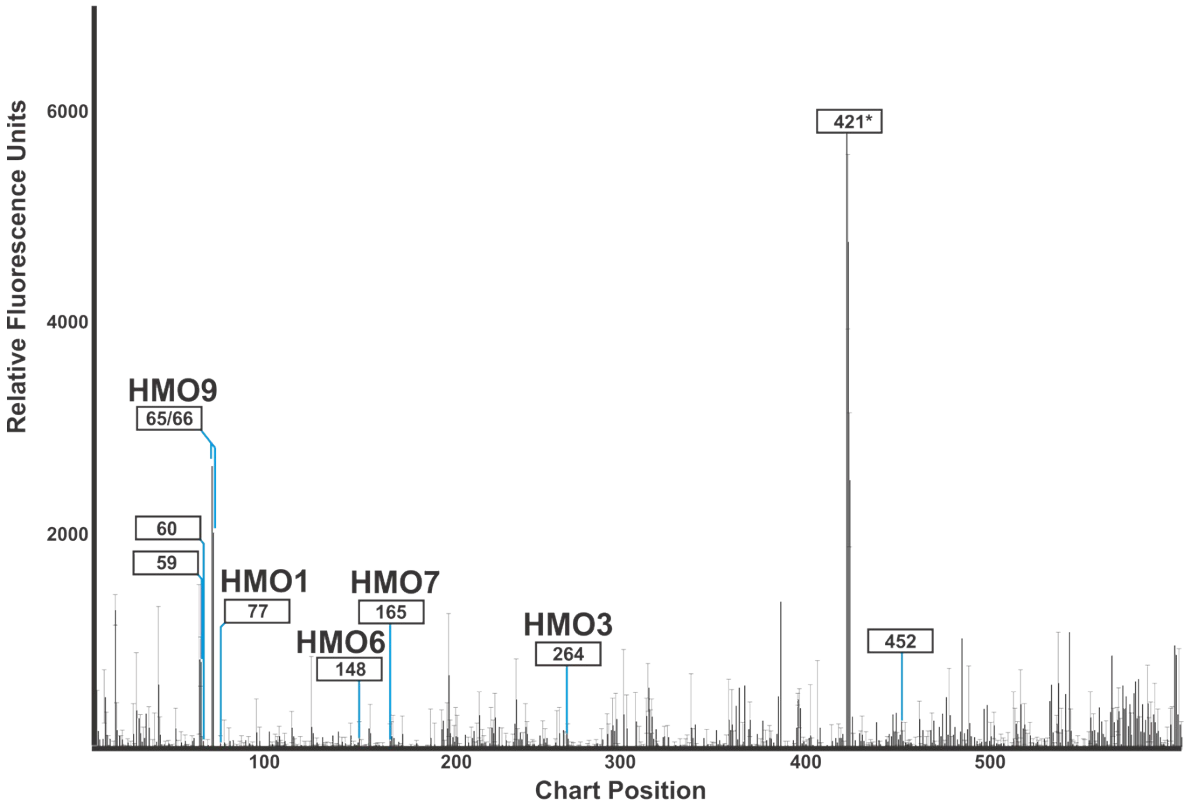

59	α-L-Fuc-(1→2)-β-D-Gal-(1→3)-β-D-GlcNAc-(1→3)-α-L-Gal-(1→4-)-β-D-Gal-(1→4)-β-D-Glc-Sp9
60	α-L-Fuc-(1→2)-β-D-Gal-(1→3)-[α- L-Fuc-(1→4)]-β-D-GlcNAc-Sp8
65	α-L-Fuc-(1→2)-β-D-Gal-(1→3)-β-D-GlcNAc-(1→3)-β-D-Gal-(1→4)-β-D-Glc-Sp8
66	α-L-Fuc-(1→2)-β-D-Gal-(1→3)-β-D-GlcNAc-(1→3)-β-D-Gal-(1→4)-β-D-Glc-Sp10
77	α-L-Fuc-(1→2)-β-D-Gal-(1→4)-β-D-Glc-Sp0
148	β-D-Gal-(1→3)-β-D-GlcNAc-(1→3)-β-D-Gal-(1→4)-β-D-Glc-Sp10
165	β-D-Gal-(1→4)-β-D-GlcNAc-(1→3)-β-D-Gal-(1→4)-β-D-Glc-Sp8
264	α-D-Neu5Ac-(2→3)-β-D-Gal-(1→4)-β-D-Glc-Sp8
421*	α-L-Fuc-(1→2)-β-D-Gal-(1→3)-β-D-GlcNAc-(1→3)-α-D-GalNAc-Sp14
452	α-D-GalNAc-(1→4)-β-D-Gal-(1→4)-β-D-Glc-Sp0

Figure S22. Results of glycan array screening (Consortium for Functional Glycomics glycan microarray version 5.2) of BabA. The structures of the modified HMOs in the array are shown, along with the structure of compound 421, which produced the highest response.

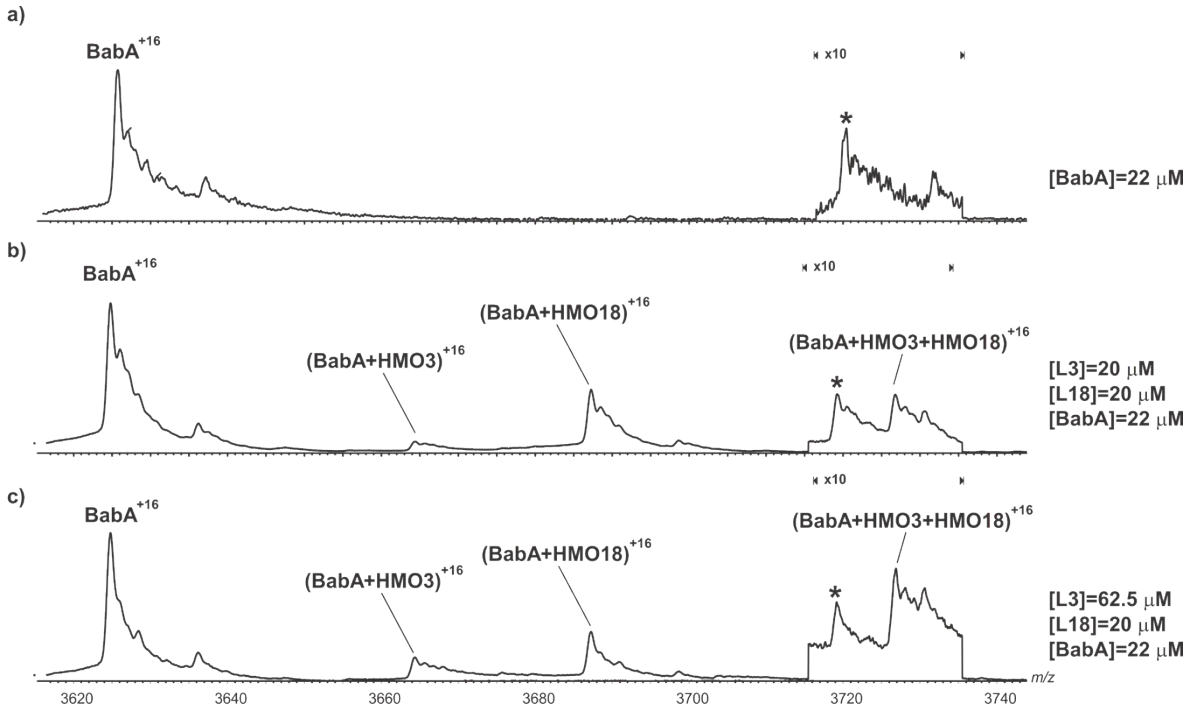

Figure S23. Representative ESI mass spectra acquired in positive ion mode for aqueous ammonium acetate solutions (20 mM, pH 6.8) of (a) BabA (22 μM) alone and with (b) **HMO3** (20 μM) and **HMO18** (20 μM) or (c) **HMO3** (62.5 μM) and **HMO18** (20 μM). * unidentified impurity.

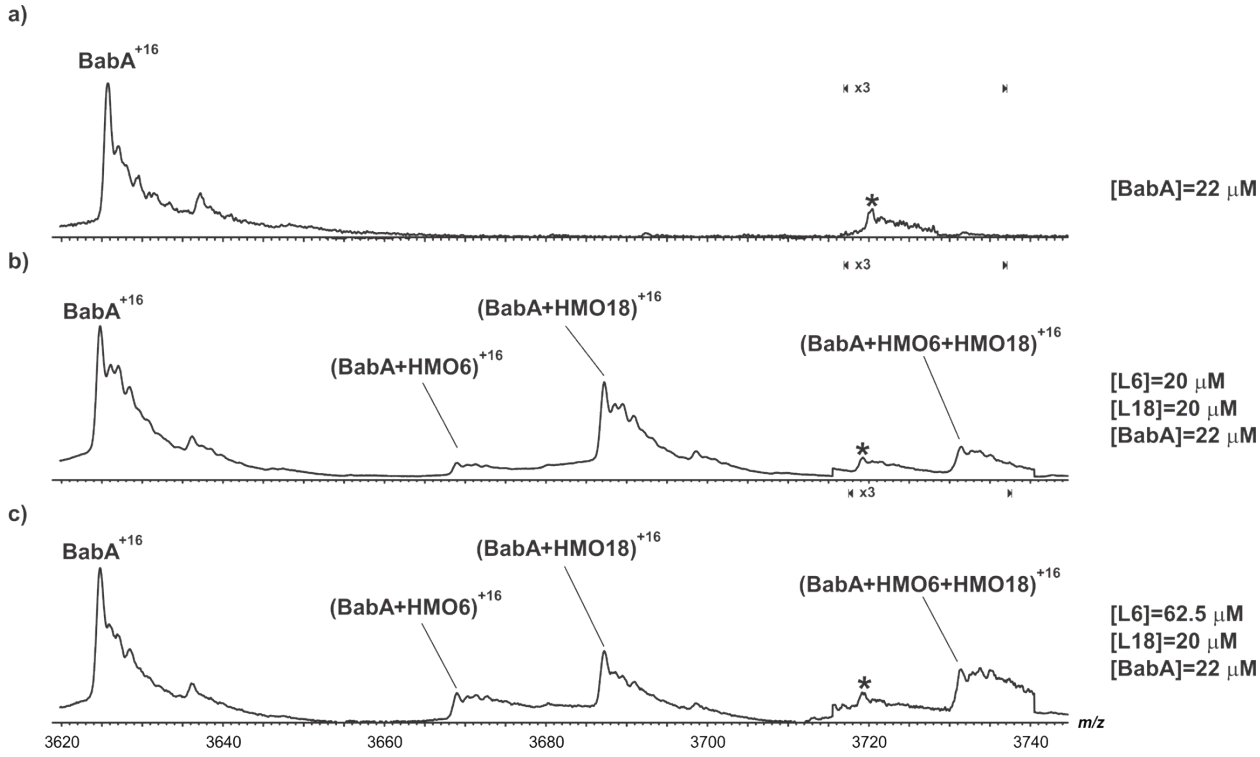

Figure S24. Representative ESI mass spectra acquired in positive ion mode for aqueous ammonium acetate solutions (20 mM, pH 6.8) of (a) BabA (22 μM) alone and with (b) **HMO6** (20 μM) and **HMO18** (20 μM) or (c) **HMO6** (62.5 μM) and **HMO18** (20 μM). * unidentified impurity.

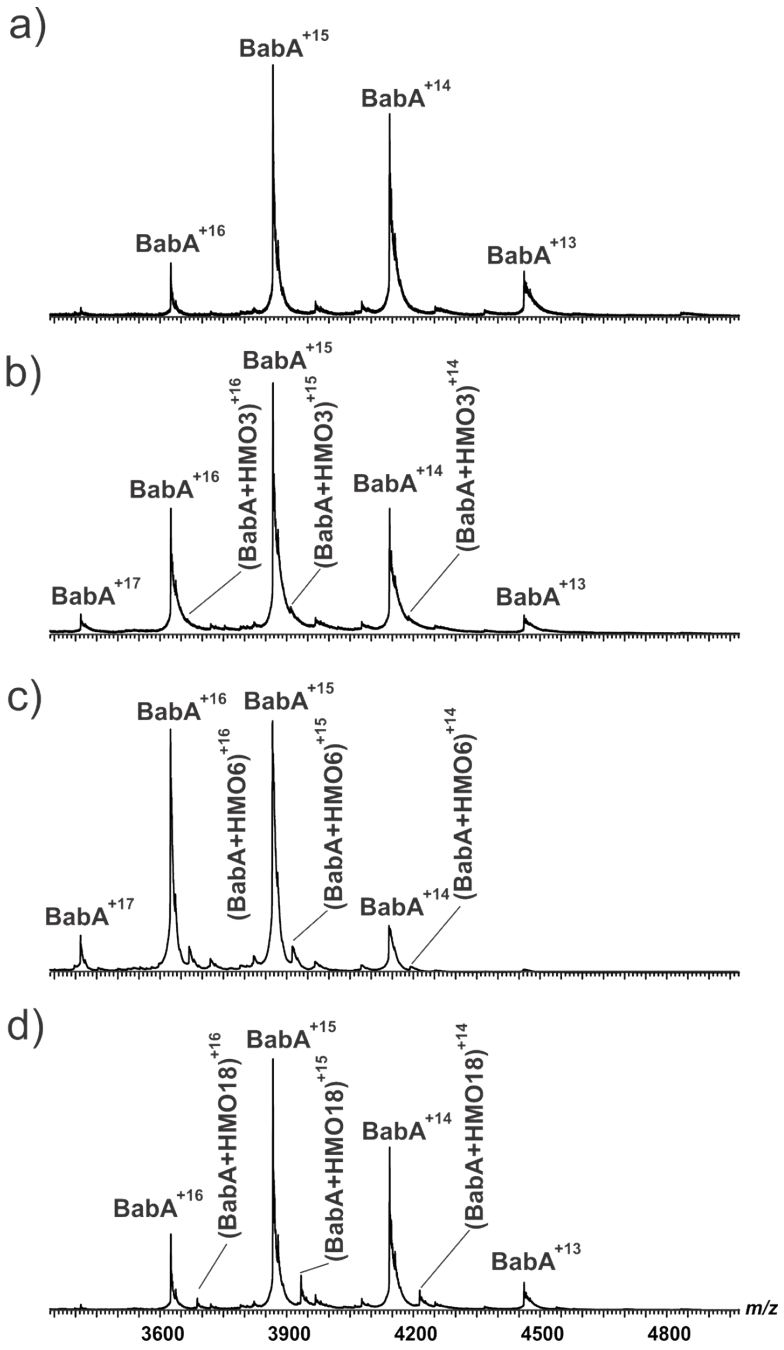

Figure S25. Representative ESI mass spectra acquired in positive ion mode for aqueous ammonium acetate solutions (20 mM, pH 6.8) of (a) BabA (20 μM) alone and with (b) **HMO3** (5 μM) or (c) **HMO6** (10 μM) or (d) **HMO18** (10 μM).

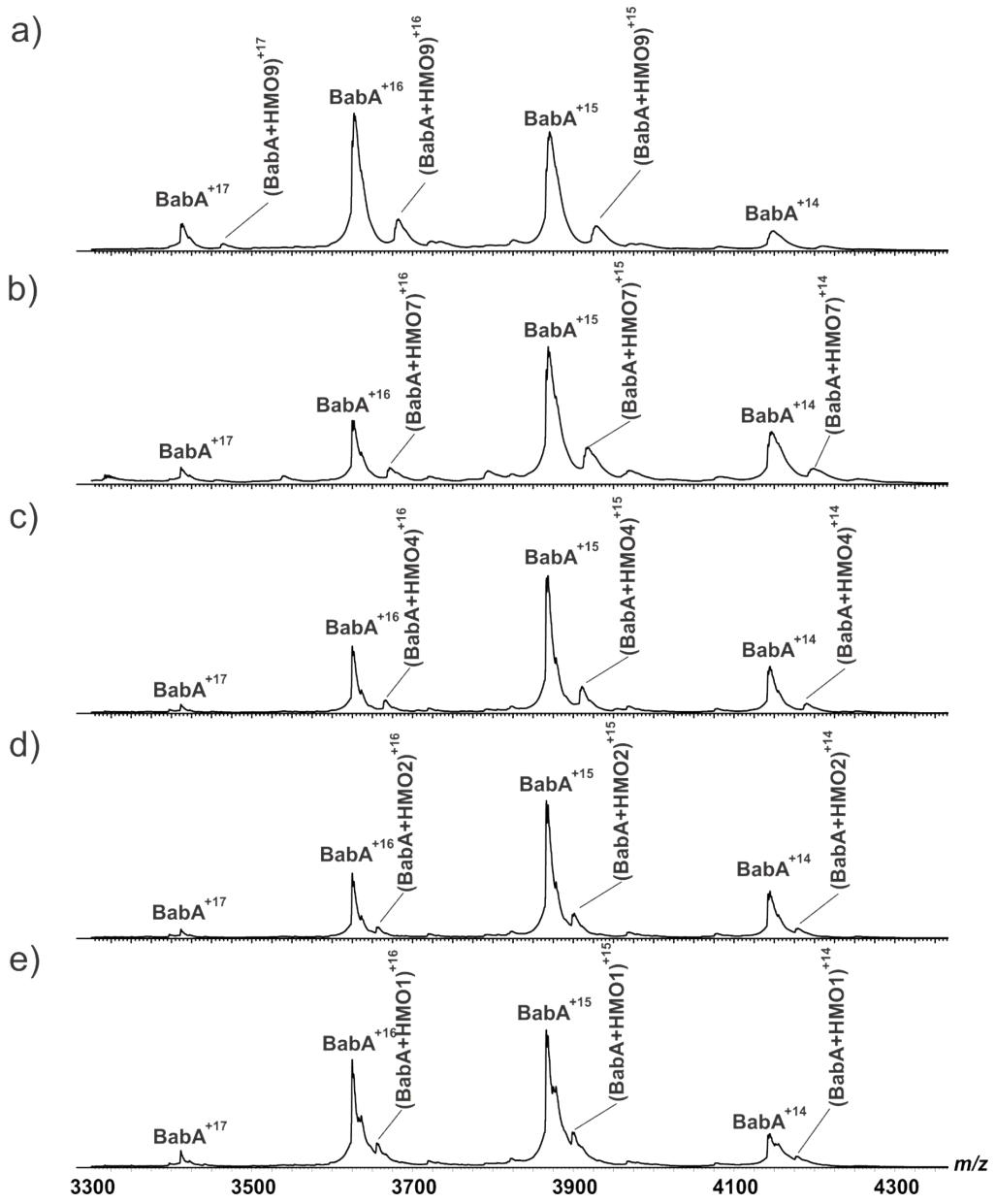

Figure S26. Representative ESI mass spectra acquired in positive ion mode for aqueous ammonium acetate solutions (20 mM, pH 6.8) of (a) BabA (20 μM) alone and with (b) **HMO3** (5 μM) or (c) **HMO6** (15 μM) or (d) **HMO18** (10 μM). (b) **HMO 9** (15 μM) or (c) **HMO7** (15 μM) or (d) **HMO4** (15 μM) or (d) **HMO2** (15 μM) or (e) **HMO1** (15 μM).